Original Article

Efficient volume-based localization and automatic labeling of intracranial depth electrodes

Baotian Zhao[1], Xuemin Zhao[1,2], Wenhan Hu[1,3,4], Chao Zhang[1], Xiu Wang[1], Jiajie Mo[1], Xiaoqiu Shao[5], Kai Zhang[1,3,4], Jianguo Zhang[1,3,4]

[1]Department of Neurosurgery, Beijing Tiantan Hospital, Capital Medical University, Beijing, China; [2]Department of Neuroelectrophysiology, Beijing Neurosurgical Institute, Beijing, China; [3]Stereotactic and Functional Neurosurgery Laboratory, Beijing Neurosurgical Institute, Capital Medical University, Beijing, China; [4]Beijing Key Laboratory of Neurostimulation, Beijing, China; [5]Department of Neurology, Beijing Tiantan Hospital, Capital Medical University, Beijing, China

Contributions: (I) Conception and design: B Zhao, K Zhang, J Zhang; (II) Administrative support: X Shao, J Zhang; (III) Provision of study materials or patients: W Hu, C Zhang, X Wang; (IV) Collection and assembly of data: X Zhao, J Mo; (V) Data analysis and interpretation: B Zhao, X Zhao; (VI) Manuscript writing: All authors; (VII) Final approval of manuscript: All authors.

Correspondence to: Jianguo Zhang. Department of Neurosurgery, Beijing Tiantan Hospital, Capital Medical University, No. 119 South 4th Ring West Road, Fengtai District, Beijing 100070, China. Email: zjguo73@126.com.

Background: The accurate localization and anatomical labeling of intracranial depth electrodes are crucial for stereoelectroencephalography (SEEG) recordings and the interpretation of results in patients with epilepsy. The laborious electrode localization procedure requires an efficient and easy-to-use pipeline. Thus, we developed a useful tool, which we called the depth electrode localizer (DELLO), to automatically identify and label depth electrode contacts with ease.

Methods: The DELLO is an open-source package developed in MATLAB (MathWorks). It was specifically fine-tuned to expedite the localization of depth electrodes. The basic procedures include preoperative magnetic resonance imaging (MRI) and postoperative computed tomography coregistration, intensity threshold electrode spatial sampling, the hierarchical clustering of electrode samples, and gray-matter and automatic anatomical labeling (AAL). The DELLO also has a graphical user interface (GUI) that can be used to review the results. The only manual intervention procedures are the identification of the target (tip) and entry point of each electrode and the naming of the clustered electrode contact groups, which generally take ~5 min per case. The coordinates of each contact were recorded in individual spaces and were also transformed in standard space by applying a volume-based deformation field. To validate the performance of the current method, 7 patients with epilepsy were retrospectively included in the analysis.

Results: A total of 80 depth electrodes, including 1,030 contacts from the 7 patients with epilepsy, were localized. All the procedures functioned well, and the entire process was robust and intuitive. Among the 1,030 contacts, 746 (72.43%) were labeled as inside the gray matter. The gray-matter and AAL accuracy rates were 95.83% and 90.78%, respectively, over all contacts.

Conclusions: The DELLO is an integrated tool that was designed to semi-automatically localize and label intracranial depth electrodes. It is open source and freely available. Given its high accuracy and efficiency, the DELLO could facilitate SEEG interpretation and be used in SEEG-based cognitive neuroscience studies.

Keywords: Epilepsy surgery; stereoelectroencephalography (SEEG); intracranial electrode; electrode localization; anatomical labeling

Submitted Jul 24, 2022. Accepted for publication Dec 03, 2022. Published online Feb 21, 2023.
doi: 10.21037/atm-22-3712
View this article at: https://dx.doi.org/10.21037/atm-22-3712

Introduction

The use of stereoelectroencephalography (SEEG) in depth electrodes, which has the advantages of being minimally invasive and capable of sampling deep structures, is gaining popularity in the presurgical evaluation process for drug refractory epilepsy (1-3). Due to its high spatial and temporal resolutions, SEEG also provides a unique research platform for cognitive neuroscience and can be used in causal studies (4,5). The precise localization of each electrode and anatomical labeling are fundamental in SEEG studies, as this information is essential for characterizing seizure onset and spreading and facilitating functional evaluations, such as presurgical cortical mapping (6-9). Clinical neuroscience researchers also need location information to explore the neural dynamics of brain regions under certain cognitive conditions (10). The accurate localization of electrodes is essential to the interpretation of results; however, the individualized localization of each electrode contact can be laborious, and on average, there are over 100 electrode contacts per patient. Furthermore, the labeling process may not be feasible for researchers with limited anatomical expertise. Overall, electrode localization information is crucial for treatment decision-making after SEEG monitoring, but currently, there are very few efficient and accurate localization techniques.

Many electrode localization methods have been developed to address the aforementioned challenges. From a modality perspective, a quick solution of electrode localization is to use the X-rays radiographs, but X-rays can only provide course localization (11). Some recent studies have performed localization based solely on magnetic resonance imaging (MRI) (12) or adopted the strategy of presurgical MRI and postoperative computed tomography (CT) coregistration (13,14), which are feasible and prevalent in clinical settings. Generally, 2 types of intracranial electrodes are currently used (i.e., subdural and depth electrodes), and current methods tend to adjust their functions by incorporating both types of electrodes (14,15). Thus, the identification of the dimensions and geographical key points can require sophisticated maneuvering, which may be time consuming. Depth electrodes are typically straight and regular in shape, and these features can be used to simplify localization procedures for depth electrodes (16). For group analyses, the conversion of the individual coordinates into a standard Montreal Neurological Institute (MNI) space is required. Given the different forms of electrodes, surface warping methods may not work well for depth electrodes (17), and volumetric warping is more suitable for depth electrodes (18). The statistical parametric mapping (SPM) toolbox (https://www.fil.ion.ucl.ac.uk/spm/ext/) provides robust volume warping methods for MRI images. Furthermore, accurate MNI space coordinate conversion enables researchers to take advantage of publicly available brain atlas and segmentation data, which are typically released in the MNI space.

To address the issues of previous studies, we designed a semiautomatic localization and fully automatic anatomical labeling (AAL) tool named the depth electrode localizer (DELLO), which is fine-tuned for intracranial depth electrode localization in a MATLAB environment. The basic steps of the pipeline include image coregistration, intensity thresholding, sample clustering, and volume-based electrode labeling. The entire process requires very few manual interventions. The DELLO performs the following functions: (I) the location of 3-dimensional (3D) coordinates in individual space, (II) the provision of coordinates in standard space using non-linear transformation, (III) the automatic labeling of electrode contacts with gray/white-matter and AAL-based tags, and (IV) a quick volume review panel that shows the localization results. The procedures are summarized as in *Figure 1*.

Highlight box

Key findings

- We developed the depth electrode localizer (DELLO), an integrated tool, to facilitate the localization and labeling of intracranial depth electrodes in patients with epilepsy.

What is known and what is new?

- Little research has been conducted on the automatic analysis of intracranial depth electrodes.
- We developed an open-source volume-based tool to localize intracranial depth electrodes that has high accuracy and efficiency.
- The reliability and robustness of the tool were tested in clinical cases.

What is the implication, and what should change now?

- The DELLO tool could facilitate stereoelectroencephalography interpretation and be used in cognitive neuroscience studies.

Methods

Patients and depth electrodes

A total of 7 patients with focal epilepsy who underwent SEEG evaluation at the Beijing Tiantan Hospital were retrospectively included in this study. Patients with

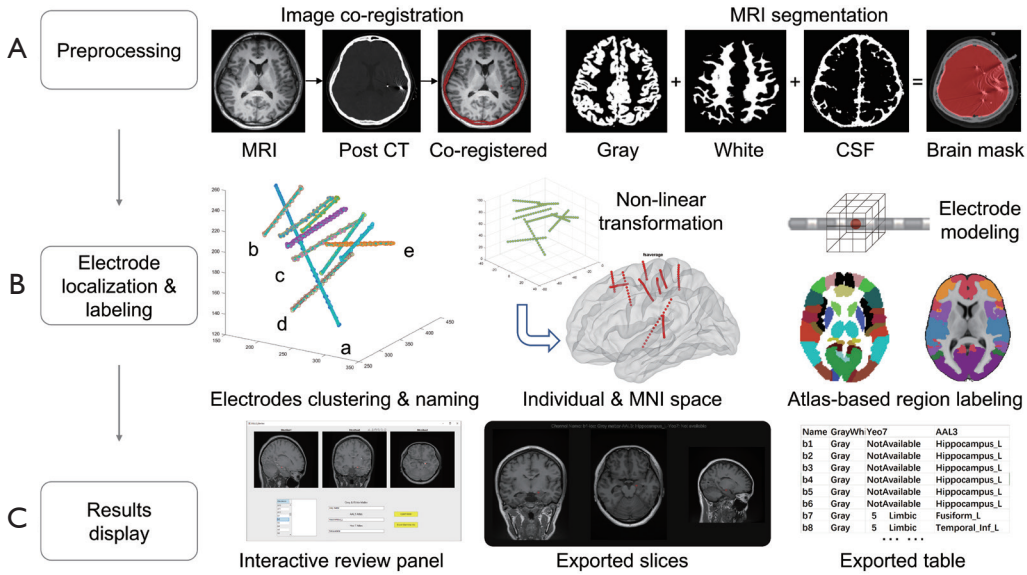

Figure 1 A diagram of the preprocessing pipeline. The basic procedures are as follows: (A) image preprocessing: the coregistration of MRI and postoperative CT scans, MRI segmentation, and brain mask generating. (B) At the electrode labeling stage, the clustered depth-electrode samples are renamed with their true labels. The native space and MNI coordinates are recorded. Electrode contact is modeled as a 3×3×3 cube, sampling its surrounding volume voxels in native (gray-matter labeling) and MNI space (AAL and Yeo7 atlas). (C) The results displaying module provides an interactive review panel, and all the results can be exported and saved as described in the results section. MRI, magnetic resonance imaging; CT, computed tomography; CSF, cerebrospinal fluid; MNI, Montreal Neurological Institute; AAL, automatic anatomical labeling.

nontumor epilepsy were selected to avoid major MRI anatomical distortions that could potentially affect segmentation and the subsequent labeling. The study was conducted in accordance with the Declaration of Helsinki (as revised in 2013). This study was approved by the Ethics Board of the Beijing Tiantan Hospital, Capital Medical University (No. KY2016-008-01). Informed consent was given by patients about the use of data for research purposes. Intracerebral multiple contact depth electrodes (8–16 contacts; length 2 mm; diameter 0.8 mm; 1.5 mm apart; Huake-Hengsheng Medical Technology, Beijing, China) were placed using a Cosman–Roberts–Wells (CRW) frame-based system (Integra Radionics, Burlington, MA, USA) to record intracranial electroencephalogram (EEG) data. The strategy for electrode placement was based on noninvasive information that provided clinical hypotheses about the localization of the epileptogenic zone (EZ).

Acquisition of MRI and CT images

The following neuroimaging protocols were used on all the participants in the study: high-resolution 3D T1-weighted magnetization prepared rapid gradient echo (T1WI MPRAGE) sequencing [repetition time (TR) 2,300 ms, echo time (TE) 2.53 ms, flip angle 12°, slice thickness 1 mm, no gap, voxel size 1 mm × 1 mm × 1 mm] with a 3T Siemens Verio scanner (Siemens Healthineers, Erlangen, Germany). CT scans (120 kVp, field of view 320 mm, matrix 512×512, slice thickness 0.625 mm; LightSpeed VCT, GE Healthcare, Chicago, IL, USA) were also obtained. The data were collected on the same day of the electrode implantation to confirm the electrode locations and prevent potential complications, such as hematoma and electrode displacement, as part of the routine clinical procedure.

MRI and CT coregistration

The MRI and CT images were first exported in (digital imaging and communications in medicine) DICOM format and then converted to (neuroimaging informatics technology initiative) NIfTI format (http://nifti.nimh.nih.gov). The CT images were coregistered to MRI images with the SPM12 toolbox using a 6-parameter rigid-body

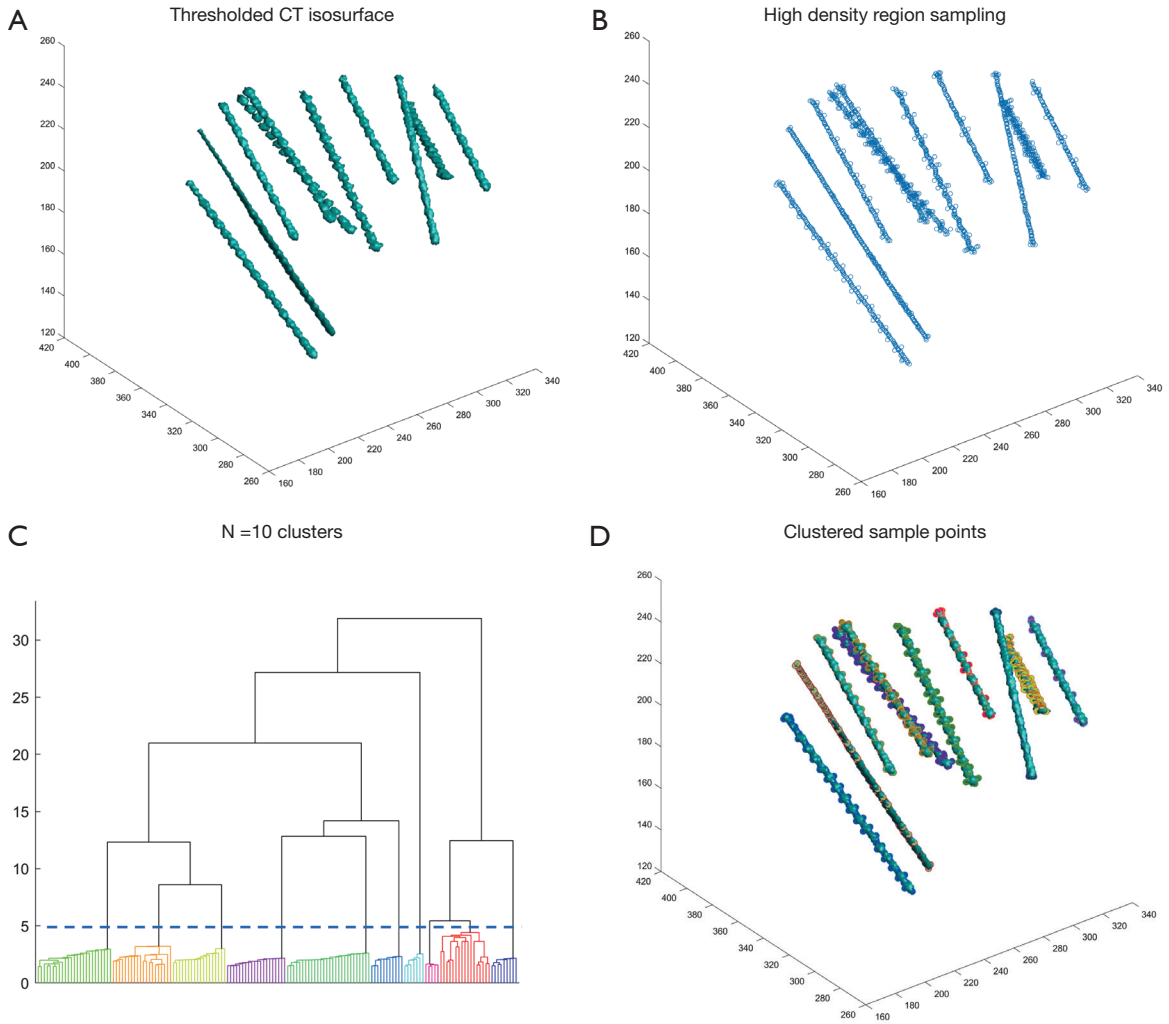

Figure 2 Electrode clustering using hierarchical clustering. (A) The isosurface plot based on the binarized CT images with the intensity threshold. (B) Depth electrode autodetection and sampling. (C) Hierarchical clustering of the electrode samples. Notably, the cluster threshold was set to be equal to the number of total electrode shafts. (D) The clustered results of sample points differentiating among the depth electrodes. CT, computed tomography.

transformation in native space based on the maximization of the normalized mutual information (19). The coregistered MRI images were resliced in alignment with the CT dimensions because the CT images has a smaller thickness. The coregistered images were saved for inspection.

Depth electrode sampling

After the image coregistration, a brain mask was generated by combining the segmented MRI components, including gray matter, white matter, and cerebrospinal fluid, in SPM12 software. The brain mask was further eroded from the outer ring in 3D to avoid unnecessary high-density clusters. The brain mask was used to exclude outside brain high-density interference by multiplying the binary mask with the CT volume. After masking, an intensity threshold was set to make a binary brain mask for displaying the depth electrodes for further sampling. By default, the CT intensity threshold was set as the 99.5% percentile of the whole-brain CT values, and a panel displaying the real-time intensity thresholding effect was displayed. The threshold could be manually modified to generate proper intensity thresholding and clustering results (*Figure 2*).

Clinically, the CT scans could have different angles. The

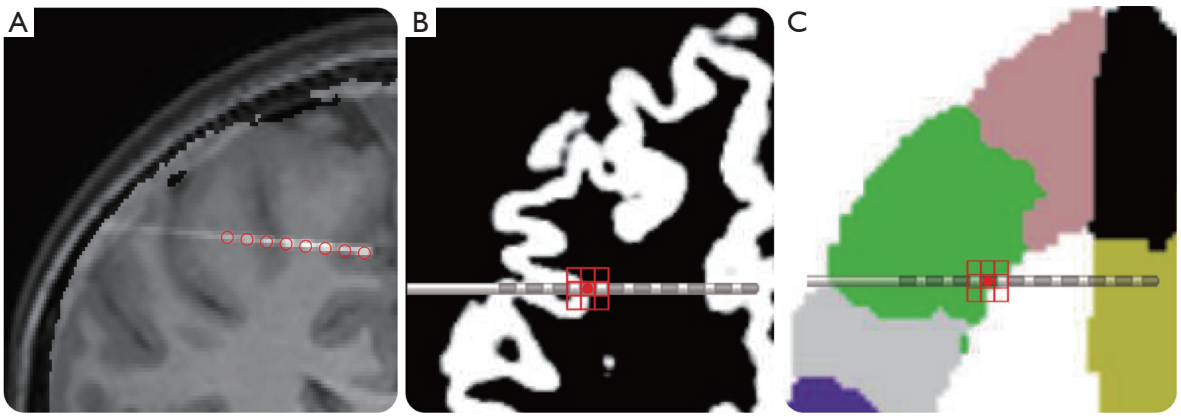

Figure 3 Case illustration of accurate contact labeling and group-level MNI space labeling results. (A) An example showing that each electrode contact was accurately localized based on the DELLO in the individual space. (B) Two-dimensional illustration depth electrode contact coverage modeling. Each contact was surrounded by a 3×3×3 mm cubic modeling. Within the virtual cubic model, the gray-matter percentage was calculated based on the individual gray-matter mask generated from SPM MRI segmentation. A threshold was then set the determine the gray/white-matter labeling of the specific contact. (C) A similar labeling procedure was used for the AAL. The specific contact was surrounded by a virtual cubic model, and the template segmentation information was counted inside the cubic model. Notably, the procedure was performed in an MNI template space. MNI, Montreal Neurological Institute; DELLO, depth electrode localizer; SPM, statistical parametric mapping; MRI, magnetic resonance imaging; AAL, automatic anatomical labeling.

depth electrode trajectory sampling was based on the binary threshold CT images and performed using the MATLAB 2D regionprops function in 3 directions separately, and the results were then combined to ensure that all the high-density voxels were properly sampled. All the sample points were used for the hierarchical clustering. Specifically, from the sample coordinates, a hierarchical cluster tree was created using the nearest Euclidean distance method. Next, clusters from the hierarchical cluster tree were constructed, starting from the root until the number of total clusters equaled the number of electrode shafts (*Figure 2*).

At this stage, each cluster of sample points corresponded to 1 electrode, and the next step was electrode labeling. Additionally, the depth electrodes were oversampled, and the exact coordinates of each contact needed to be specified. In this study, as all the depth electrodes were essentially straight, we only needed to define the target (the tip), entry (the contacts close to the skull), and the electrode specification, including the number of contacts and intercontact space, which were adjustable through the parameter control script to accommodate electrodes of different specifications.

To facilitate the labeling, we built a graphical user interface (GUI) panel with a sliding bar to select and display samples in each cluster. The panel represents the only part of the whole localization procedure that requires manual maneuvering. This procedure typically takes ~5 minutes if the labeler is familiar with the general location of each electrode. Using such information, all the contacts within 1 electrode could be calculated through trigonometric equations. As the target and entry points were located within the clustered sample points, the key points could simply be selected by browsing through the existing points. Finally, the coordinates of each contact in the individual space were recorded. The above-mentioned procedures are summarized in *Figure 1*. The open-source codes are freely available online (https://github.com/zhaobaotian/DELLO).

Electrode labeling

Gray-matter labeling was performed in the individual space to ensure its accuracy. With the MRI and CT coregistered images (*Figure 3A*), a binary gray-matter mask was produced using the SPM12 segmentation procedure with a threshold of 0.1. A 3×3×3 voxel cube centered on the contacts was modeled to sample the surrounding voxels. The contact was labeled as outside the gray matter if the 3×3×3 voxel cube contained fewer than a certain number of gray-matter voxels (*Figure 3B*). The default threshold was 9 voxels, but it could be adjusted to modify the strictness of the gray-matter electrode inclusion.

For brain atlas-based anatomical labeling, before the

anatomical labeling, the individual coordinates were transformed into MNI space. Given that all the depth electrodes were located inside the brain parenchyma, we conducted a nonlinear transformation of the coordinates using the normalization function in SPM12. In brief, a deformation field was created during the transformation of the structural MRI to standard space, and a nonlinear deformation field was applied to all the coordinates. The labeling through the brain templates was similar to the subsequent gray-matter labeling (*Figure 3C*). It is possible that 1 contact sampled different parcellations in the atlas; in such cases, the contact was assigned to the brain region with more voxel sampling. In the default setting, we selected 2 representative atlases for the brain region labeling; that is, the AAL (20) and Yeo7 atlas (21). We also provided a programmable interface that was compatible with any volume-based brain atlas. The MNI coordinates and anatomical labeling results were recorded.

Manual validation of automatic labeling results

The localization and labeling results were saved in comma-separated values (CSV) format. To facilitate further review, we created a panel that enabled the interactive selection and browsing of the results.

The localization of each contact should be theoretically precise, but automatic electrode labeling may be inaccurate given the precision loss during space normalization and course parcellation from the atlas. Thus, we manually examined the accuracy by reviewing the gray/white-matter and anatomical labeling results. A senior neurosurgeon (WH) reviewed all the data to determine whether the DELLO had properly assigned each contact to certain brain regions. To further avoid the potential bias introduced by the DELLO anatomical labeling, 2 senior neurosurgeons (KZ and CZ), who were blind to the algorithm results, independently labeled each contact according to the AAL atlas definitions. Any discrepancies were resolved by discussion. The functional parcellation based on the Yeo7 atlas was not evaluated because the functional networks lack clear anatomical boundaries for human visual judgement.

Statistical analysis

The judgement and labeling of the expert were adopted as the gold standard. The accuracy percentage of electrode labeling for each patient was recorded. The basic patient demographic and electrode implantation information were provided.

Results

The DELLO tool

The entire pipeline was developed in a MATLAB environment (Video S1). Each case had an independent folder containing 3 files as input. The input files were organized as follows: (I) the presurgical MRI data, which were converted to the NIfTI format and renamed *3DT1.nii*; (II) the postoperative CT images, which were in NIfTI format and named *postCT.nii*; and (III) patient's electrode information, which included 2 columns saved in CSV format. The first column corresponded to the name of each electrode, and the second column recorded the number of contacts. We provided a data input panel for selecting the proper files (*Figure 4A*).

The preprocessing procedures (as described in the method section), typically took approximately 10 min for a 4-core 3.6-GHz central processing unit with 16-GB random access memory without manual intervention. Next, a CT intensity threshold window was used to manually check the high-intensity clustering (*Figure 4B*). If the results were not satisfactory, the thresholding value was changed to optimize the high-density sampling results. After depth electrode sampling and clustering were performed, the user took advantage of the electrode naming panel to assign tags for each cluster (*Figure 5*). For each contact, 3 directions of volume view were shown. The electrode name, target point, and entry point were consecutively defined through the GUI panel. As not all the clustering was perfect (e.g., in rare cases, the samples from 1 depth electrodes were assigned to 2 different clusters), we also designed a manual correction mechanism that provided sample point correction with large freedom, and alternatively, the users could also choose other samples in a given electrode shaft as the tip point or entry point After all the electrodes had been named and the 2 key points defined, the procedure performed the automatic labeling.

Result reviewing the export

For each subject, the DELLO tool automatically generated intermediate files during the process for further visual inspection, such as the brain mask. The key result output comprised the following 4 files: (I) the electrode name files, which comprised the name of each contact; (II)

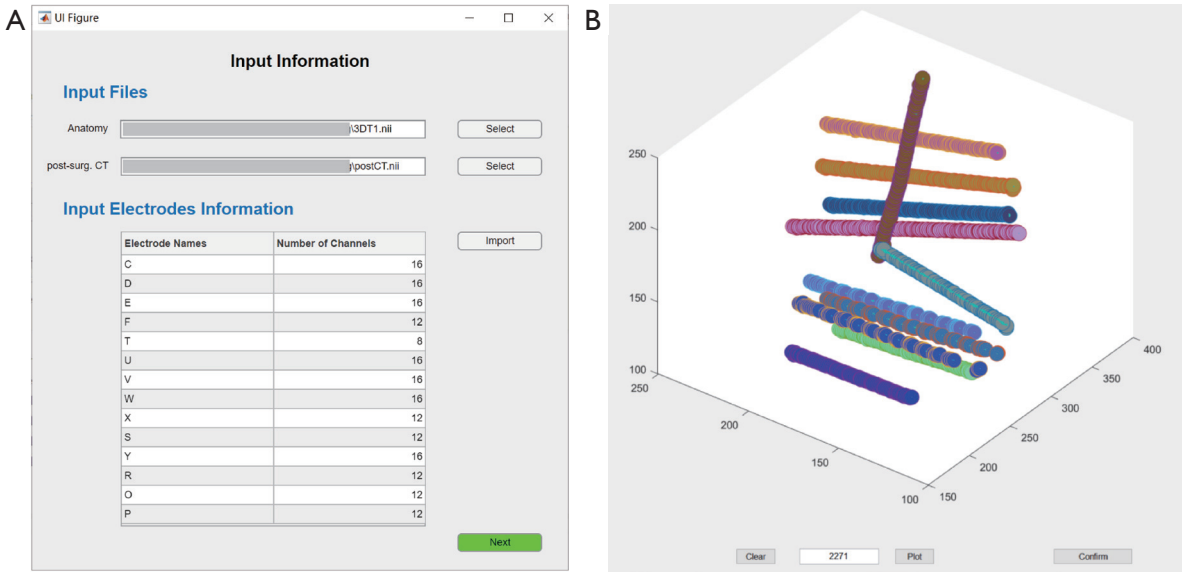

Figure 4 Input and CT intensity thresholding panel. (A) A GUI panel was used to select the input data. (B) A CT intensity thresholding panel showing ideal clustering with a proper threshold. The threshold was adjustable though the panel, and the results could be displayed after changing the threshold value for inspection. CT, computed tomography; GUI, graphical user interface.

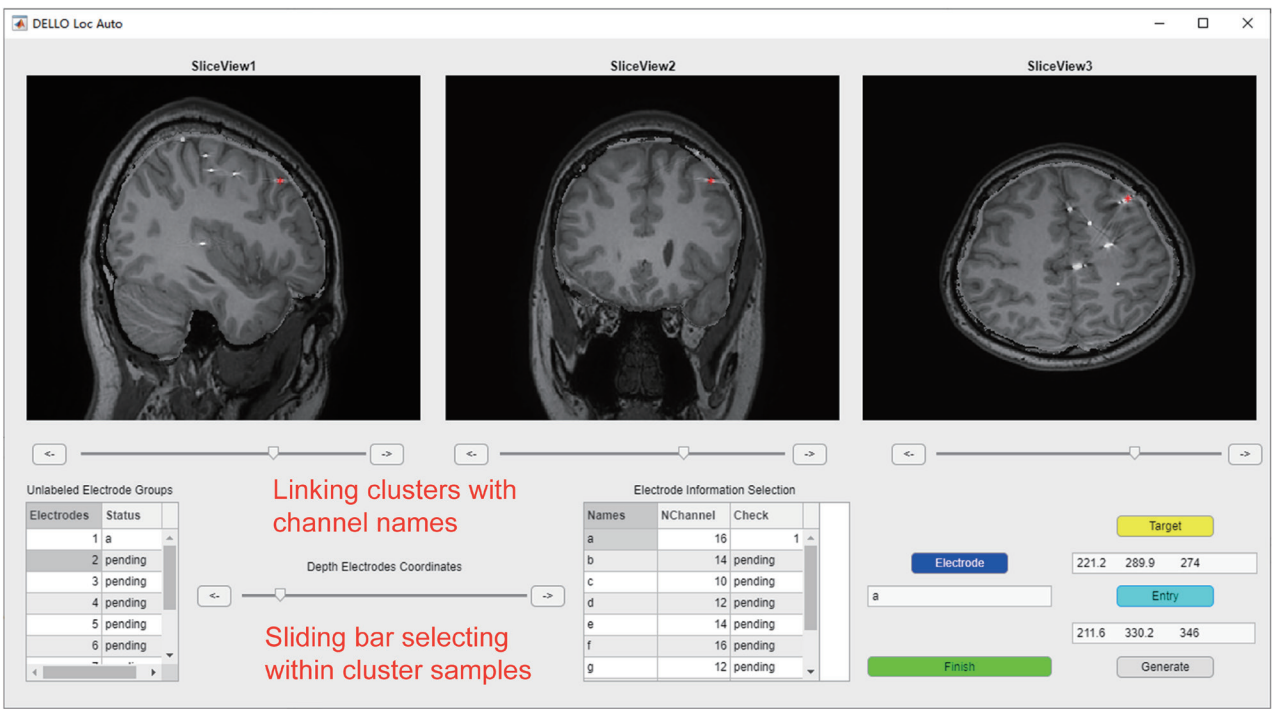

Figure 5 Electrode naming panel. Users should select the matched cluster groups and the electrode name cells to rename the specific electrode shaft. The sliding bar is used to select samples within 1 electrode shaft and define the target and entry points. The coordinates of each contact are calculated.

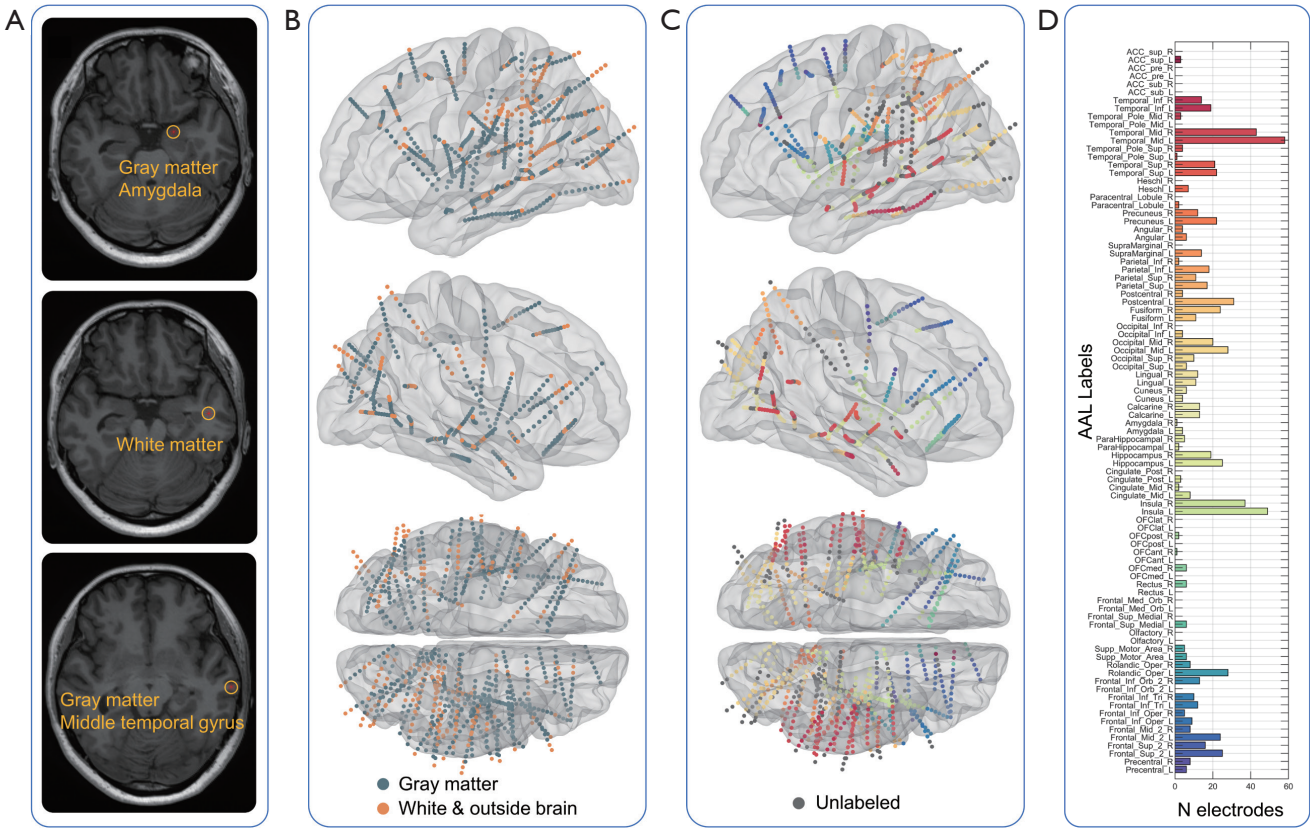

Figure 6 Single- and group-level electrode labeling result examples. (A) Automatic labeling results for 2-dimensional slices. (B) The grouped electrodes and gray-matter labeling of 80 electrodes for the 7 patients. (C) The group-level AAL labeling results. The 3D visualization was assisted by the iELVis toolbox (13). (D) The anatomical distribution of the 1,030 contacts from the 7 patients based on the AAL atlas parcellations. AAL, automatic anatomical labeling; ACC, anterior cingulate cortex; iELVis, intracranial electrode visualization.

the corresponding coordinates in individual space using the MRI as the coordinate base; (III) the MNI space coordinates; and (IV) the contact labels, including gray/white-matter, AAL, and Yeo7 atlas tags. All the results were saved as text files. To facilitate the result visualization, a review panel was built to enable the user to interactively select the specific contact needed (Figure S1). These positions are shown in the individual space. In addition, the image results could be exported as slices for each contact.

Patient and electrode distribution

The data of 7 patients (3 females and 4 males) with an average age of 19.5 years (range, 10–34 years) were analyzed. A total of 80 electrodes with 1,030 contacts were localized and labeled bilaterally across all brain lobes (*Figure 6*). The basic information of the cohort is presented in Table S1. In general, the localization process using the DELLO was smooth and stable, and the localization accuracy was satisfactory.

Automatic labeling accuracy

We manually validated the labeling results of the gray-matter and AAL labels. Given that the gray-matter labeling was performed in native space, it is not surprising that the gray-matter electrode labeling achieved higher accuracy than did the AAL labeling (on average 95.83% *vs.* 90.78%). The gray-matter/AAL labeling accuracy rates across patients were consistent (95.45%/90.91%, 98.61%/89.58%, 92.21%/94.81%, 97.06%/84.56%, 94.83%/86.21%, 96.88%/94.79%, and 95.51%/91.67% respectively). The match rates between the automatic labeling and independent blind gray/AAL labeling for each patient were 84.85%/75.00%, 81.94%/79.86%, 85.06%/75.97%, 79.41%/78.68%, 87.07%/81.90%, 91.67%/88.54%, and

83.97%/80.13%, respectively, and the average match rates were 85.15% and 80.39%, respectively, indicating acceptable accuracy. The gray- and AAL manual labeling for 100 contacts took the experienced specialist ~30 min.

The gray-matter electrodes were mainly mislabeled due to morphological MRI changes, such as electrodes being located inside the abnormal periventricular heterotopia; thus, SPM12 segmentation could not parcellate the gray-matter mask with satisfactory results. In addition, gray-matter segmentation might also have been affected by low-contrast MRI structural images. In a few cases, AAL labeling errors were observed, which might have been partially due to the coarse volume mask we chose, which did not account for the morphology of the matter. Some of the mesial temporal structures, such as the amygdala, were also mislabeled, which might have been due to their irregular morphology. When we filtered the results to include only the gray-matter electrodes, the AAL labeling accuracy increased to 95.84%. Using the output gray- and white-matter labels, the users easily filtered out the contacts of interest. We recommend that the AAL labels be filtered using gray-matter masks.

Discussion

The accurate localization and labeling of intracranial electrodes are essential for epilepsy presurgical evaluations and cognitive neuroscience studies. We developed a semiautomatic pipeline specifically designed for depth electrodes that was shown to be both accurate and easy to use. The localization procedure relied on the assumption that all the depth electrodes were spatially straight and that all the contacts were localized based on basic key points and electrode dimensions. The anatomical labeling was atlas-based and used the SPM normalization deformation field, which is suitable for volume-based coordinate transformation. Overall, the gray-matter and AAL labeling accuracy rates for the 1,030 SEEG contacts were 95.83% and 90.78%, respectively.

Currently, several toolboxes are available for localizing intracranial electrodes, each of which has its own advantages. From the neuroimage modality perspective, Yang *et al.* used postimplantation MRI and developed a method for localizing electrode arrays (12). Other common methods coregister postoperative CT with presurgical MRI scans, as CT scans are routinely performed after the implantation at centers and are time efficient (17,22,23). In relation to the specific localization methods, most studies have adopted manual or semiautomatic methods that, for example, label each of the electrodes (15) or key corners of the grid arrays (18) to avoid sampling errors from threshold CT images. Notably, Blenkmann *et al.* developed an electrode autodetection method using the CT high-intensity signal (24). However, under such methods, spurious nonelectrode voxels need to be considered and manually removed as necessary.

To address the CT artifact issues, we first applied an eroded brain mask to exclude any irrelevant volumes. We then assumed that all the depth electrodes were straight so that only 2 key points defined the tip and entry, and combining the dimension of each electrode would be sufficient to model each contact. Additionally, the linearity assumption avoided unnecessary jitters and fit the realistic contact distribution well. All the high-intensity voxels should be properly sampled; however, a name still needs to be assigned to each cluster manually, but this process was greatly facilitated by the DELLO GUI.

To achieve surface-based localization and 3D visualization, some methods have integrated Freesurfer (25) brain surface procedures. However, surface-based electrode localization and warping may be less optimal than volume-based approach for depth electrodes. In addition, brain surface reconstruction can take hours, and users need to switch between different toolboxes, which increases the probability of incorrect operations (22). Based on the MNI coordinates created by the DELLO, the 3D positions and the 3D brain models can also be visualized, which is especially suitable for group analyses.

Several studies have examined the use of algorithms in depth electrode localization. For example, Davis *et al.* developed the locate electrodes graphical user interface (LeGUI) toolbox, which has a user-friendly interface and an anatomical labeling accuracy rate of 94% (26). Narizzano *et al.* integrated the 3D slicer platform SEEG assistant (27) in another tool that enables the 3D visualization of the depth electrodes. Narizzano *et al.*'s tool, which uses fast automated stereo-EEG electrode contact identification and labeling ensemble (FASCILE) written in Python, had a <1 mm localization error and was used to manually identify, sort, and label electrode contacts in ~10 min (28). Other techniques, such as EpiTools (29) and toolbox by Wang *et al.* (14), have adopted similar workflows for depth electrode reconstruction. In addition, the commercially available multimodal neuroimaging software CURRY (Compumedics Limited) includes an intracranial EEG analysis module. Compared to the above-mentioned tools,

the DELLO seeks to localize the depth electrode with an optimized efficient workflow. To do this, additional CT high-density sampling and clustering are employed to further increase the automatic degree of the algorithm. As a result, the reviewer manual operating time was minimized as much as possible, and the efficiency was further boosted without compromising the accuracy.

Compared to subdural electrodes (30,31), depth electrodes have several advantages, including being less invasive, providing better coverage of the deep structures, and having lower complication rates. These advantages have boosted the prevalence of SEEG in recent years (31). Clinically, any SEEG results should be interpreted in relation to the anatomical information, as the depth electrodes are implanted according to the anatomo–electro–clinical correlations working hypothesis (32). Seizure onset and an early propagation zone raise special concerns, as they are closely related to the EZ. Additionally, depicting the functional eloquent cortex is essential in guiding surgical resection. All the above-mentioned processes require highly precise electrode localization.

Anatomical annotations of each contact are meaningful, given the anatomical parcellations, and are typically associated with specific neurological functions. This is especially true for group analyses, as using a common atlas, the seizure dynamics can be described properly with precision. Traditional manual labeling requires high expertise and takes considerable time. The DELLO tool uses labeling processes that can be automatically completed with high accuracy. Given that the reliability of gray-matter labeling is high we recommend filtering the electrode within the gray matter before adopting AAL labels.

Extensive intracranial EEG studies have been conducted in the cognitive neuroscience field (33,34). SEEG studies are characterized by high spatial and temporal resolutions in certain brain regions. Due to the spatial sampling restrictions of individual patients, researchers tend to perform group-level analyses in standard MNI space, which require robust electrode coordinate warping to preserve the topology properties. The DELLO addresses such issues by providing labeled anatomical sites and MNI coordinates. The DELLO also provides raw localization data that can be used in other visualization tools, such as intracranial electrode visualization (13), brainstorm (35), and EEGLAB (36).

The current version of the DELLO has several limitations. First, the DELLO was designed solely for depth electrode localization; thus, it may not be suitable for subdural electrodes without modification. Second, the proposed method does not address electrode intersection and bending issues. Third, the interspace of the depth electrode should be identical, and to locate other types of depth electrodes, the user must change the parameters. Finally, additional steps, including neuroimage format conversion and other possible data correction, were not integrated in the pipeline. These issues will be addressed in future updated versions of the DELLO.

Conclusions

In this study, we developed an integrated tool to localize and label depth electrodes that can be used in intracranial EEG research. The DELLO provides a streamlined pipeline; has high accuracy, robustness, efficacy, and simplicity; and can facilitate depth electrode localization and labeling across all brain regions in patients with epilepsy. The DELLO is a practical tool that can assist in both the clinical diagnosis of patients and in intracranial EEG research.

Acknowledgments

Funding: This study was supported by National Natural Science Foundation of China (Nos. 82201600, 82271495, 82071457 and 82201603), National Key R&D Program of China (No. 2021YFC2401201), Capital's Funds for Health Improvement and Research (Nos. 2022-1-1071, 2020-2-1076).

Footnote

Data Sharing Statement: Available at https://atm.amegroups.com/article/view/10.21037/atm-22-3712/dss

Peer Review File: Available at https://atm.amegroups.com/article/view/10.21037/atm-22-3712/prf

Conflicts of Interest: All authors have completed the ICMJE uniform disclosure form (available at https://atm.amegroups.com/article/view/10.21037/atm-22-3712/coif). The authors have no conflicts of interest to declare.

Ethical Statement: The authors are accountable for all aspects of the work in ensuring that questions related to the accuracy or integrity of any part of the work are appropriately investigated and resolved. This study was conducted in accordance with the Declaration of Helsinki

(as revised in 2013). The study was approved by the Ethics Committee of the Beijing Tiantan Hospital (No. KY2016-008-01) and informed consent was taken from all the patients.

References

1. Bulacio JC, Chauvel P, McGonigal A. Stereoelectroencephalography: Interpretation. J Clin Neurophysiol 2016;33:503-10.
2. Bartolomei F, Lagarde S, Wendling F, et al. Defining epileptogenic networks: Contribution of SEEG and signal analysis. Epilepsia 2017;58:1131-47.
3. Zhao B, Zhang C, Wang X, et al. Orbitofrontal epilepsy: distinct neuronal networks underlying electroclinical subtypes and surgical outcomes. J Neurosurg 2020. [Epub ahead of print]. doi: 10.3171/2020.5.JNS20477.
4. Veit MJ, Kucyi A, Hu W, et al. Temporal order of signal propagation within and across intrinsic brain networks. Proc Natl Acad Sci U S A 2021;118:e2105031118.
5. Liu Y, Shi G, Li M, et al. Early top-down modulation in visual word form processing: Evidence from an intracranial SEEG study. J Neurosci 2021;41:6102-15.
6. Drane DL, Pedersen NP, Sabsevitz DS, et al. Cognitive and Emotional Mapping With SEEG. Front Neurol 2021;12:627981.
7. Bartolomei F, Chauvel P, Wendling F. Epileptogenicity of brain structures in human temporal lobe epilepsy: a quantified study from intracerebral EEG. Brain 2008;131:1818-30.
8. Grinenko O, Li J, Mosher JC, et al. A fingerprint of the epileptogenic zone in human epilepsies. Brain 2018;141:117-31.
9. Parvizi J, Kastner S. Promises and limitations of human intracranial electroencephalography. Nat Neurosci 2018;21:474-83.
10. Kucyi A, Daitch A, Raccah O, et al. Electrophysiological dynamics of antagonistic brain networks reflect attentional fluctuations. Nat Commun 2020;11:325.
11. Miller KJ, Makeig S, Hebb AO, et al. Cortical electrode localization from X-rays and simple mapping for electrocorticographic research: The "Location on Cortex" (LOC) package for MATLAB. J Neurosci Methods 2007;162:303-8.
12. Yang AI, Wang X, Doyle WK, et al. Localization of dense intracranial electrode arrays using magnetic resonance imaging. Neuroimage 2012;63:157-65.
13. Groppe DM, Bickel S, Dykstra AR, et al. iELVis: An open source MATLAB toolbox for localizing and visualizing human intracranial electrode data. J Neurosci Methods 2017;281:40-8.
14. Qin C, Tan Z, Pan Y, et al. Automatic and Precise Localization and Cortical Labeling of Subdural and Depth Intracranial Electrodes. Front Neuroinform 2017;11:10.
15. Li G, Jiang S, Chen C, et al. iEEGview: an open-source multifunction GUI-based Matlab toolbox for localization and visualization of human intracranial electrodes. J Neural Eng 2019;17:016016.
16. Deman P, Bhattacharjee M, Tadel F, et al. IntrAnat Electrodes: A Free Database and Visualization Software for Intracranial Electroencephalographic Data Processed for Case and Group Studies. Front Neuroinform 2018;12:40.
17. Trotta MS, Cocjin J, Whitehead E, et al. Surface based electrode localization and standardized regions of interest for intracranial EEG. Hum Brain Mapp 2018;39:709-21.
18. Hamilton LS, Chang DL, Lee MB, et al. Semi-automated Anatomical Labeling and Inter-subject Warping of High-Density Intracranial Recording Electrodes in Electrocorticography. Front Neuroinform 2017;11:62.
19. Ken S, Di Gennaro G, Giulietti G, et al. Quantitative evaluation for brain CT/MRI coregistration based on maximization of mutual information in patients with focal epilepsy investigated with subdural electrodes. Magn Reson Imaging 2007;25:883-8.
20. Rolls ET, Huang CC, Lin CP, et al. Automated anatomical labeling atlas 3. Neuroimage 2020;206:116189.
21. Yeo BT, Krienen FM, Sepulcre J, et al. The organization of the human cerebral cortex estimated by intrinsic functional connectivity. J Neurophysiol 2011;106:1125-65.
22. Taylor KN, Joshi AA, Hirfanoglu T, et al. Validation of semi-automated anatomically labeled SEEG contacts in a brain atlas for mapping connectivity in focal epilepsy. Epilepsia Open 2021;6:493-503.
23. Sun K, Wang H, Bai Y, et al. MRIES: A Matlab Toolbox for Mapping the Responses to Intracranial Electrical Stimulation. Front Neurosci 2021;15:652841.

24. Blenkmann AO, Phillips HN, Princich JP, et al. iElectrodes: A Comprehensive Open-Source Toolbox for Depth and Subdural Grid Electrode Localization. Front Neuroinform 2017;11:14.
25. Dale AM, Fischl B, Sereno MI. Cortical surface-based analysis. I. Segmentation and surface reconstruction. Neuroimage 1999;9:179-94.
26. Davis TS, Caston RM, Philip B, et al. LeGUI: A Fast and Accurate Graphical User Interface for Automated Detection and Anatomical Localization of Intracranial Electrodes. Front Neurosci 2021;15:769872.
27. Narizzano M, Arnulfo G, Ricci S, et al. SEEG assistant: a 3DSlicer extension to support epilepsy surgery. BMC Bioinformatics 2017;18:124.
28. Ervin B, Rozhkov L, Buroker J, et al. Fast Automated Stereo-EEG Electrode Contact Identification and Labeling Ensemble. Stereotact Funct Neurosurg 2021;99:393-404.
29. Medina Villalon S, Paz R, Roehri N, et al. EpiTools, A software suite for presurgical brain mapping in epilepsy: Intracerebral EEG. J Neurosci Methods 2018;303:7-15.
30. Tantawi M, Miao J, Matias C, et al. Gray Matter Sampling Differences Between Subdural Electrodes and Stereoelectroencephalography Electrodes. Front Neurol 2021;12:669406.
31. Joswig H, Lau JC, Abdallat M, et al. Stereoelectroencephalography Versus Subdural Strip Electrode Implantations: Feasibility, Complications, and Outcomes in 500 Intracranial Monitoring Cases for Drug-Resistant Epilepsy. Neurosurgery 2020;87:E23-30.
32. Chauvel P, Gonzalez-Martinez J, Bulacio J. Presurgical intracranial investigations in epilepsy surgery. Handb Clin Neurol 2019;161:45-71.
33. Lachaux JP, Axmacher N, Mormann F, et al. High-frequency neural activity and human cognition: past, present and possible future of intracranial EEG research. Prog Neurobiol 2012;98:279-301.
34. Rizzolatti G, Fabbri-Destro M, Caruana F, et al. System neuroscience: Past, present, and future. CNS Neurosci Ther 2018;24:685-93.
35. Tadel F, Baillet S, Mosher JC, et al. Brainstorm: a user-friendly application for MEG/EEG analysis. Comput Intell Neurosci 2011;2011:879716.
36. Delorme A, Makeig S. EEGLAB: an open source toolbox for analysis of single-trial EEG dynamics including independent component analysis. J Neurosci Methods 2004;134:9-21.

(English Language Editors: L. Huleatt and J. Gray)

Cite this article as: Zhao B, Zhao X, Hu W, Zhang C, Wang X, Mo J, Shao X, Zhang K, Zhang J. Efficient volume-based localization and automatic labeling of intracranial depth electrodes. Ann Transl Med 2023;11(6):242. doi: 10.21037/atm-22-3712

Supplementary

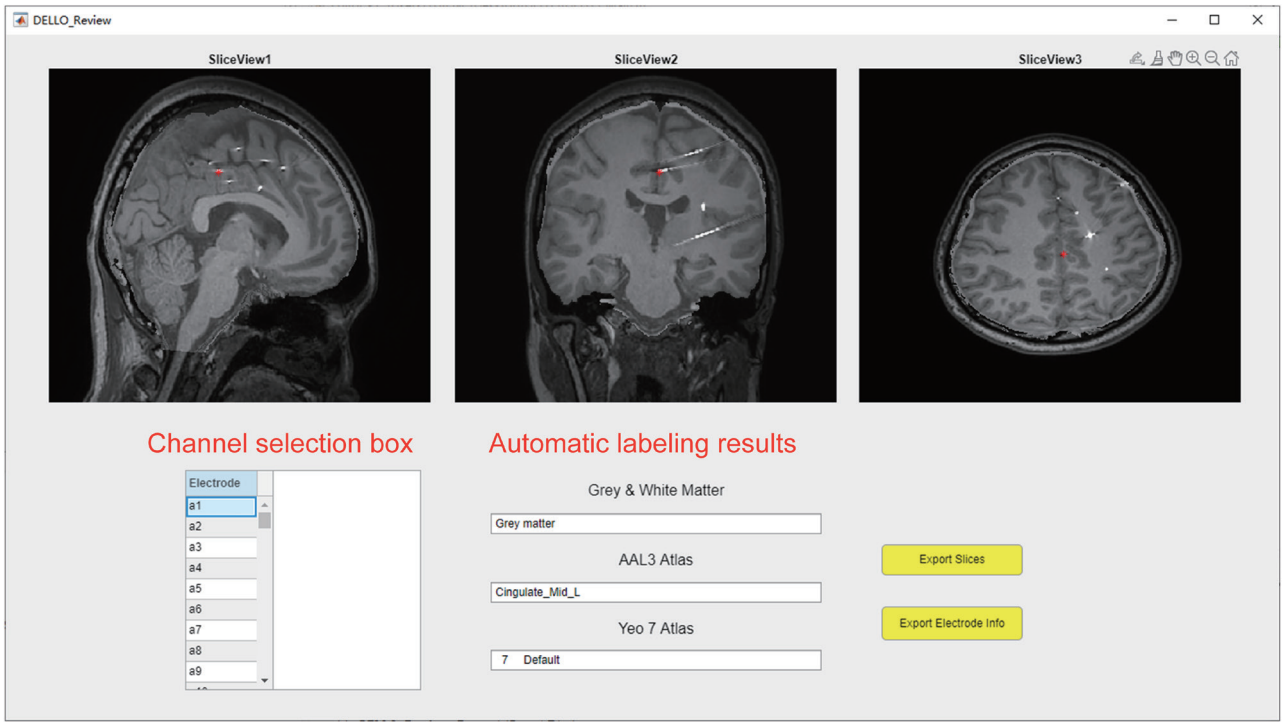

Figure S1 An electrode reviewing panel displaying localization and labeling results in an interactive manner.

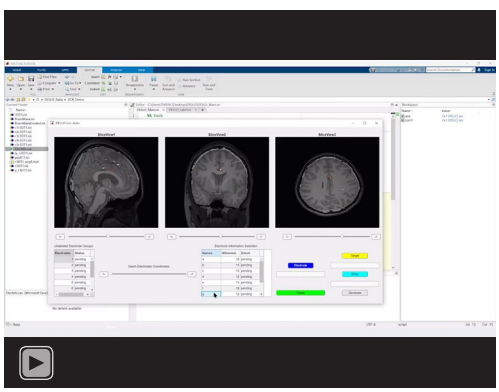

Video S1 Screen capture video demonstrating the basic workflow of electrode localization and labeling.

https://dx.doi.org/10.21037/atm-22-3712

Table S1 Clinical information of the7 patients

Cases	Gender/age (years)	Depth electrode (contacts × #)	Side	Brain area				
				F	T	P	O	I
01	M/10	16 × 1; 12 × 9; 8 × 1	B		1	5	5	
02	F/14	16 × 3; 12 × 8	B	3				8
03	F/32	16 × 4; 14 × 4; 12 × 2; 10 × 1	L		7	3		1
04	M/13	16 × 7; 12 × 2	R		2	1	5	1
05	F/34	16 × 1; 14 × 1; 12 × 4; 10 × 3; 8 × 1	R	1	6	1	1	1
06	M/14	16 × 7; 12 × 6; 8 × 1	L		4	6	3	1
07	M/20	16 × 1; 12 × 9; 8 × 4	L	8		2		4

M: male; F: female; L: left; R: right; B: bilateral; N: number of electrodes; F: frontal; T: temporal; P: parietal; O: occipital; I: insula.

https://dx.doi.org/10.21037/atm-22-3712